

ARE THE ULTRA-FAINT DWARF GALAXIES JUST CUSPS?

ADI ZOLOTOV¹, DAVID W. HOGG¹, BETH WILLMAN²,

(Dated: October 12, 2010)

To be submitted for publication in *ApJ*

ABSTRACT

We develop a technique to investigate the possibility that some of the recently discovered ultra-faint dwarf satellites of the Milky Way might be cusp caustics rather than gravitationally self-bound systems. Such cusps can form when a stream of stars folds, creating a region where the projected 2-D surface density is enhanced. In this work, we construct a Poisson maximum likelihood test to compare the cusp and exponential models of any substructure on an equal footing. We apply the test to the Hercules dwarf ($d \sim 113$ kpc, $M_V \sim -6.2$, $e \sim 0.67$). The flattened exponential model is strongly favored over the cusp model in the case of Hercules, ruling out at high confidence that Hercules is a cusp catastrophe. This test can be applied to any of the Milky Way dwarfs, and more generally to the entire stellar halo population, to search for the cusp catastrophes that might be expected in an accreted stellar halo.

Subject headings: Galaxy — halo; galaxies — dwarfs

1. INTRODUCTION

In the last five years, a number of ultra-faint Milky Way satellites have been discovered with one millionth of the Milky Way’s luminosity or less. These objects have stars with $[\text{Fe}/\text{H}]$ at least as low as -3.0 , $[\text{Fe}/\text{H}]$ spreads of up to 1 dex (Kirby et al. 2008; Frebel et al. 2010; Simon et al. 2010), and velocity dispersions of $\sim 3 - 7$ km sec⁻¹ (Simon & Geha 2007) despite scale sizes of 30 - 200 pc (Martin et al. 2008). The best explanation for these observed properties thus far is that we are observing dwarf galaxy member stars moving on bound orbits within highly dark matter dominated potential wells. Within this scenario, the velocity dispersions of these objects imply mass-to-light ratios of 10^{2-4} within their central 300 pc (Strigari et al. 2008) and that galaxies can form with total luminosities of only $\sim 1000L_\odot$ - far less than the luminosities of some individual stars.

These remarkable conclusions should require a high burden of proof: Are there any other plausible explanations for the ultra-faint Milky Way satellites as a population? One possibility is that the ultra-faints could have intrinsic near-zero velocity dispersions (on thus no dark matter), but that binary stars have inflated their observed dispersions. While this scenario could be conceivable for a small number of objects, it cannot explain away the entire ultra-faint galaxy population (Simon et al. 2010; Martinez et al. 2010; McConnachie & Côté 2010). Moreover, the low amount of and large spread in their iron abundances show that these objects cannot have formed in the same way as globular clusters, ruling out (disrupting) globular cluster scenarios. The possible inflated ellipticities of ultra-faint dwarfs relative to their more luminous neighbors (Martin et al. 2008) combined with claims of irregular isophotes tempts a conclusion that these are tidal remnants. However, claims of isophote irregularity have been inconclusive for the

majority of ultra-faint satellites. Recently, Martin & Jin (2010) have found that the shape of the Hercules dwarf might be explained by tidal disruption.

A fourth possibility is that (a subset of) the kinematically cold, spatial overdensities that we have identified as ultra-faint galaxies are instead cusp caustics of cold stellar debris. Cold substructures, a subset of which may be two dimensional and sheet-like, are both observed (e.g. Grillmair 2006; Yanny et al. 2003; Belokurov et al. 2006) and predicted to be abundant in the Milky Way’s halo. Sheet structures can form generically when leading and trailing streams from a tidally disrupted satellite wrap the Galaxy to make a sheet-like shell. Shells have been seen in both simulations (Hernquist & Quinn 1988) and observations (Malin & Carter 1983) of early-type galaxies. A sheet of stars that bends can produce visible fold caustics (“catastrophes”), cusp caustics, and higher-order caustics in the observed two-dimensional distribution of stars (Tremaine 1999). A cusp caustic in a two-dimensional observable space appears as a highly elliptical centroid of stars where two fold caustics meet. In this scenario, some of the ultra-faint dwarfs may actually be cusps and some of the cold streams could be folds.

In this paper, we develop a technique for testing the hypothesis that ultra-faint dwarf galaxies are the 2-D projections of such folded stellar sheets. We apply this technique to the Hercules Milky Way satellite, which has $d \sim 113$ kpc, $M_V \sim -6.2$, and $e \sim 0.67$ (Sand et al. 2009). We choose this object because it has the highest ellipticity of any of the Milky Way’s dwarfs and is thus a good candidate for the cusp model.

2. OBSERVATIONAL DATA

Coleman et al. (2007, hereafter C07) obtained Large Binocular Telescope imaging of the Hercules dwarf galaxy in the Gunn r band (25 minutes), V band (20 minutes), and B band (30 minutes) to derive its structural parameters. The Large Binocular Camera spans a $23' \times 23'$ field of view. C07 applied color-color-magnitude filtering in colors c_1 and c_2 (combinations of r , V , and B) to their point source catalog to select objects most consistent with belonging to Hercules rather than to the

¹ Center for Cosmology and Particle Physics, Department of Physics, New York University, 4 Washington Place, New York, NY 10003; az481@nyu.edu

² Haverford College, Department of Astronomy, 370 Lancaster Avenue, Haverford, PA 19041

field. In this paper we utilize the $\sim 10,000$ stars from the C07 CMD selected subset of their LBT/LBC Hercules catalog. This catalog is identical to what they used to derive the structure of Hercules. Please see C07 for further details on this data set.

3. MODEL COMPARISON: CUSP VS EXPONENTIAL

We aim to determine whether a cusp model is a better explanation of the spatial distribution of the elongated Hercules dwarf than a flattened exponential model. To perform this model comparison, we specify each model explicitly, compute the Poisson likelihood of the data given the models, and use the maximum likelihood of each model to determine which best fits the data.

3.1. Constructing the Models

Both of the exponential and cusp models tested here have six free parameters. The cusp model's free parameters are: central RA and Dec, rotation angle and scale, a smoothing scale, and a constant background level. The exponential model's free parameters are: central RA and Dec, a rotation angle, ellipticity, half-light radius, and a constant background level. For each model we step through the six parameters (Θ) and evaluate the likelihood of the data given each model. The full likelihood, which is a product of the individual star likelihoods, is:

$$\mathcal{L}(\Theta) = \prod_{i=1}^{N_{star}} \frac{1}{Z(\Theta)} \Sigma(x_i | \Theta) \quad (1)$$

$$Z(\Theta) = \frac{1}{N_{random}} \sum_{j=1}^{N_{random}} \Sigma(x_{random,j} | \Theta) \quad (2)$$

where Θ is the list of parameters for the cusp or exponential model, $\Sigma(\cdot)$ is the surface density of the model given the parameters, and $Z(\Theta)$ is a normalization constant, estimated using a spatially randomized stellar catalog over the observed sky region. N_{star} is the total number of stars, and \mathbf{x}_i is the two-dimensional position (on the sky) of star i . N_{random} is the total number of random points, set to equal N_{star} , and $\mathbf{x}_{random,j}$ is the position of random point j .

3.1.1. The Cusp Model

The cusp surface density model is computed following the work of Tremaine (1999). First, a background-free Σ_{cusp} is computed on a grid in the natural coordinate system ξ :

$$\Sigma_{cusp}(\xi_1, \xi_2) = \sum_{roots} \left[1 + \frac{1 + y^2}{(\xi_2 + 3y^2)^2} \right]^{1/2}, \quad (3)$$

where

$$\xi_1 = -y^3 - \xi_2 y. \quad (4)$$

In three dimensions, coordinates ξ_1 and ξ_2 make up the 2-D observable space, while coordinate y is the third, and hidden, dimension. As a third degree polynomial, equation (4) has either one or three solutions, depending on the position in ξ . Equation (3) is to be summed over all the possible roots of variable y , obtained by solving equation (4). In regions where there is no cusp, there will only

be one solution to equation (4), and hence no summation in the calculation of the surface density is necessary. On the other hand, in regions of ξ where there is a cusp, the variable y will be triple valued, and equation (3) must be summed over all three roots. Because this function has a large dynamic range, we compute it on a fine grid of 1000×1000 pixels, and use an adaptive sampling that sets the number of samples per pixel to a constant multiple of the value of the function. This essentially ensures that we are sampling more in the most interesting regions of the image, where the cusp is present. Σ_{cusp} has no free parameters in the natural coordinate system.

After the cusp image has been computed on a grid, it is smoothed with a symmetric two-dimensional Gaussian kernel with variance σ^2 . We have computed seven cusp models, each with a different smoothing scale, with values of $\sigma = [1, 2, 4, 8, 16, 32, 64]$ pixels. The two dimensional positions \mathbf{x}_i (RA,Dec) of each star i on the sky is converted to a position ξ_i in the natural coordinate system of the cusp model by a shift, scale and rotation:

$$\xi_i = \mathbf{R} \cdot [\mathbf{x}_i - \mathbf{X}], \quad (5)$$

where \mathbf{R} is a 2×2 matrix encoding the two free parameters of scale and rotation, and \mathbf{X} represents the two free parameters that shift the position of the center of the model on the sky. Finally the surface density Σ computed at point ξ_i is the sum of the background free Σ_{cusp} , and a constant background level Σ_{bg} :

$$\Sigma(\xi) = \Sigma_{cusp}(\xi) + \Sigma_{bg}. \quad (6)$$

3.1.2. The Exponential Model

We follow the same procedure for the exponential model as for the cusp model. The exponential model, in its natural units, is:

$$\Sigma_{exp}(\xi) = \exp(-|\xi|), \quad (7)$$

and the model is not smoothed at all. The 2×2 matrix \mathbf{R} used in this case is a symmetric tensor of scale and shear with three free parameters, used to calculate the position angle (θ), ellipticity (ϵ), and scale radius (r_h) of the model.

All models have been defined on grids of 1000×1000 pixels, on the interval $\xi = [-5, 5]$, and have six degrees of freedom. Figure 1 shows the surface brightness grids for cusp models with $\sigma = [1, 2, 4, 8]$ pixels and for the exponential model, each in their natural units.

3.2. MCMC

We use a Markov Chain Monte Carlo (MCMC) method to calculate the maximum likelihood of each model, and its corresponding parameters. MCMC simulates the likelihood for a set of parameters by sampling from the posterior distribution through a series of random draws. We specifically use the Metropolis-Hastings Algorithm, which generates a random walk and steps through each parameter in such a way that more probable values of parameter space are more often stepped to. For both the cusp and exponential models we choose a separable prior that is flat in center position (\mathbf{X}), flat in the components of the \mathbf{R} matrix, and flat in the background level (Σ_{bg}), with a lower limit of zero. There were no derivatives in our prior at the peaks in the likelihood, so it does not

Maximum Likelihood Parameters			
Parameter	Measured	Uncertainty	$\ln \mathcal{L}$
Best Exponential Profile			
R.A. (h m s)	16:31:03.9	8''	382
DEC (d m s)	+12:47:10	7''	
r_h (arcmin)	5.3	0.4	
ϵ	0.65	0.03	
θ (degrees)	-75.6	2.1	
Best Cusp Profile			
R.A. (h m s)	16:31:30	17''	280
DEC (d m s)	+12:46:15	4''	
scale ^a	37.6	2.1	
θ (degrees)	-78.1	3.1	
σ (pixels)	2	–	

^aarcmin per coordinate distance measured in ξ

affect any of our results. The acceptance ratios for all parameters are ~ 0.5 . Though less computationally efficient, this method is similar to the maximum likelihood technique used by (Martin et al. 2008) to determine the structural parameters of dwarf galaxies, and is better at escaping local minima.

3.3. Results

We find that a flattened exponential model is a far better fit to the Hercules data than any of the seven cusp models tested in this work. Of the seven cusp models tested, the cusp with a smoothing scale of $\sigma = 2$ pixels (0.75 arcmin) was found to be the most probable. The difference between the maximum likelihood of the exponential and best fit cusp model is

$$\mathcal{L}_{\text{expo}}/\mathcal{L}_{\text{cusp}} = e^{-102}. \quad (8)$$

Nominally this rules out the best cusp model in favor of the exponential at a confidence level of $> 99.99\%$.

Table 1 lists the parameters at maximum likelihood for the exponential and best cusp models. The structural parameters for the exponential model yield a position angle for Hercules at -76° , and an ellipticity of 0.65 (defined as $\epsilon = 1 - b/a$), both in good agreement with the findings of Coleman et al. (2007), Martin et al. (2008), and Sand et al. (2009). The parameters that maximize the likelihood of the cusp model are such that the model is slightly smoothed, and highly scaled. This is not surprising since the cusp model is a poor fit to the data, and at its optimal configuration it will be smoothed and scaled in such a way to resemble an flattened exponential-like distribution near the center. If Hercules were a 2-D projection of a cusp, the spatial distribution of its stars would show a highly elongated center of stars, along with two “tails” indicative of the two fold catastrophes. Figure 2 shows the predicted spatial distribution of stars for the best fit exponential and cusp models.

While the cusp model is strongly ruled out in favor of a flattened exponential, we make no claims that the exponential profile is the best available model for Hercules. We are, however, certain that since the cusp model is less favorable than the exponential, then it is also less favorable than the King (King 1966) and Plummer (Plummer 1911) profiles.

4. CONCLUSION & DISCUSSION

It has been suggested that some of the ultra-faint dwarf satellites of the Milky Way may be the 2-D projection of cusp caustics, and not gravitationally bound galaxies.

The highly elliptical Hercules dwarf is a good candidate for testing the cusp model, which predicts a highly elongated centroid of stars. We have established a hypothesis test in order to determine whether the Hercules overdensity is better modeled with a cusp or an exponential, and rule out at very high confidence the possibility that Hercules is a cusp catastrophe. While other surface brightness models have been fit to Hercules data, such as the King and Plummer profiles, we have chosen to not test such models here, and so have not evaluated how they compare to the flattened exponential model. Our intention in this work is not to advocate that an exponential profile is the best explanation of the observed ellipticity of Hercules, but rather to definitively remove from consideration the possibility that Hercules is a cusp caustic.

The work outlined in this paper can be used to test any of the Milky Way dwarfs suspected of being cusps. The highly elliptical dwarfs Ursa Major I and II are interesting candidates for such a test, though both lack obvious evidence of the double spatial tail indicative of the fold caustics that meet at the cusp. We believe that a similar hypothesis test on these galaxies will likely rule out the cusp model at a high level of confidence. Furthermore, the cusp caustic predicts triple-valued velocities for stellar members of the cusp. Spectroscopic data of the ultra-faint dwarfs suspected of being cusps can thus be used to further rule out or confirm such hypotheses.

The techniques introduced in this paper can be further extended to implement a search for cusp and fold caustics on the entire sky, using data from a large survey like the Sloan Digital Sky Survey (SDSS), *Gaia*, or the Large Synoptic Survey Telescope (LSST). Stellar streams and dwarf galaxies, which can be thought of, respectively, as one and (blurry) zero dimensional objects in phase space, have been found with multi-band two-dimensional angular maps in photometric surveys, such as SDSS. Such data sets are two-dimensional, though some distance information can be determined at low signal-to-noise using colors, and are well suited for finding low dimensional structures. Given the number of streams already known in the Milky Way’s stellar halo, it is likely that higher dimensional structures in six-dimensional phase space exist, but have not yet been found in current data (Tremaine 1999). Future surveys that return full (or nearly full) phase-space information, such as the *Gaia* mission (Perryman et al. 2001), will be much better suited than current surveys for finding systems with higher dimensionality. Meanwhile, such structures may only be easily identifiable in photometric data if their projection into 2-D observable space creates regions of enhanced density, like the cusp and fold caustics.

We thank Niayeshi Afshordi for inspiring this paper, and thank Matt Coleman for sharing the catalog of data used in Coleman et al. (2007). We also thank James Bullock for helpful comments on an earlier draft of this work. AZ and BW thank NSF AST-090844 for support. BW also thanks NSF AST-0908193 for support. DWH was partially supported by NASA NNX08AJ48G and the NSF AST-0908357.

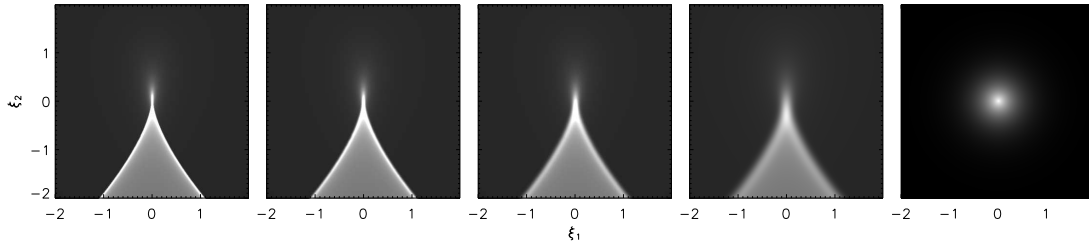


FIG. 1.— From left to right: The surface brightness maps produced by cusp models smoothed with a Gaussian kernel of variance $\sigma = [1, 2, 4, 8]$ pixels and by an exponential model, as described in Section 3.1. Each was calculated on a 1000 x 1000 pixel grid, and is plotted in its natural coordinate system, ξ .

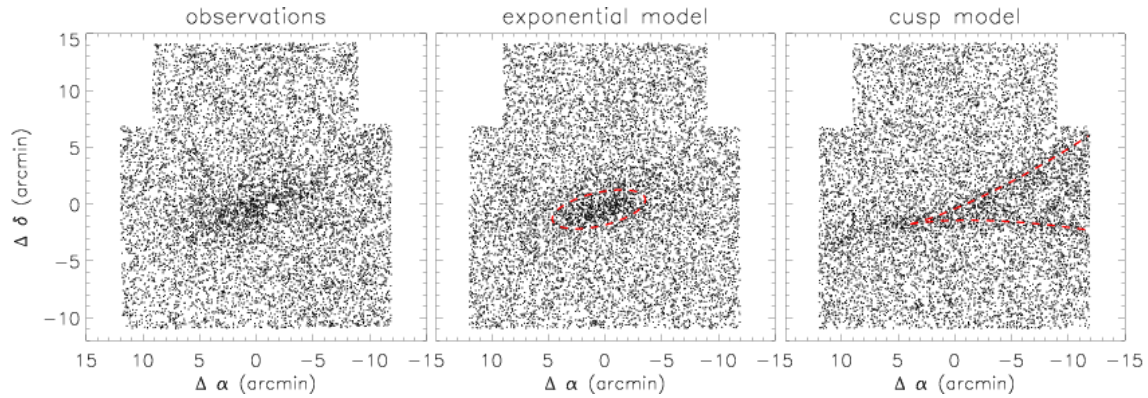


FIG. 2.— Left Panel- The observed data set of Hercules stars from Coleman et al. (2007). The elongated spatial distribution of this overdensity have raised questions as to whether it is a bound dwarf galaxy or a cusp fold. Middle Panel- The predicted spatial distribution of stars in the exponential model. Right Panel- The predicted spatial distribution of stars in the cusp model with the highest likelihood (smoothed with $\sigma = 2$ pixels). The dashed red lines mark the best fit exponential and cusp models in middle and left panels, respectively.

REFERENCES

- Belokurov, V., Zucker, D. B., Evans, N. W., Gilmore, G., Vidrih, S., Bramich, D. M., Newberg, H. J., Wyse, R. F. G., Irwin, M. J., Fellhauer, M., Hewett, P. C., Walton, N. A., Wilkinson, M. I., Cole, N., Yanny, B., Rockosi, C. M., Beers, T. C., Bell, E. F., Brinkmann, J., Ivezić, Ž., & Lupton, R. 2006, *ApJ*, 642, L137
- Coleman, M. G., de Jong, J. T. A., Martin, N. F., Rix, H., Sand, D. J., Bell, E. F., Pogge, R. W., Thompson, D. J., Hippelein, H., Giallongo, E., Ragazzoni, R., DiPaola, A., Farinato, J., Smareglia, R., Testa, V., Bechtold, J., Hill, J. M., Garnavich, P. M., & Green, R. F. 2007, *ApJ*, 668, L43
- Frebel, A., Simon, J. D., Geha, M., & Willman, B. 2010, *ApJ*, 708, 560
- Grillmair, C. J. 2006, *ApJ*, 645, L37
- Hernquist, L., & Quinn, P. J. 1988, *ApJ*, 331, 682
- King, I. R. 1966, *AJ*, 71, 64
- Kirby, E. N., Simon, J. D., Geha, M., Guhathakurta, P., & Frebel, A. 2008, *ApJ*, 685, L43
- Malin, D. F., & Carter, D. 1983, *ApJ*, 274, 534
- Martin, N. F., de Jong, J. T. A., & Rix, H. 2008, *ApJ*, 684, 1075
- Martin, N. F., & Jin, S. 2010, *ArXiv e-prints*
- Martinez, G. D., Minor, Q. E., Bullock, J., Kaplinghat, M., Simon, J. D., & Geha, M. 2010, *ArXiv e-prints*
- McConnachie, A. W., & Côté, P. 2010, *ApJ*, 722, L209
- Perryman, M. A. C., de Boer, K. S., Gilmore, G., Høg, E., Lattanzi, M. G., Lindegren, L., Luri, X., Mignard, F., Pace, O., & Zeeuw, P. T. 2001, *A&A*, 369, 339
- Plummer, H. C. 1911, *MNRAS*, 71, 460
- Sand, D. J., Olszewski, E. W., Willman, B., Zaritsky, D., Seth, A., Harris, J., Piatek, S., & Saha, A. 2009, *ApJ*, 704, 898
- Simon, J. D., & Geha, M. 2007, *ApJ*, 670, 313
- Simon, J. D., Geha, M., Minor, Q. E., Martinez, G. D., Kirby, E. N., Bullock, J. S., Kaplinghat, M., Strigari, L. E., Willman, B., Choi, P. I., Tollerud, E. J., & Wolf, J. 2010, *ArXiv e-prints*
- Strigari, L. E., Bullock, J. S., Kaplinghat, M., Simon, J. D., Geha, M., Willman, B., & Walker, M. G. 2008, *Nature*, 454, 1096
- Tremaine, S. 1999, *MNRAS*, 307, 877
- Yanny, B., Newberg, H. J., Grebel, E. K., Kent, S., Odenkirchen, M., Rockosi, C. M., Schlegel, D., Subbarao, M., Brinkmann, J., Fukugita, M., Ivezić, Ž., Lamb, D. Q., Schneider, D. P., & York, D. G. 2003, *ApJ*, 588, 824